Effect of Group-14 and Group-16 Substitution on the Photophysics of Structurally Related Donor–Acceptor Polymers

ARTICLE *in* THE JOURNAL OF PHYSICAL CHEMISTRY C · AUGUST 2013

Impact Factor: 4.77 · DOI: 10.1021/jp405257r

3 AUTHORS, INCLUDING:

Theresa M Mccormick
Portland State University
27 PUBLICATIONS **1,169** CITATIONS
SEE PROFILE

Dwight Seferos
University of Toronto
88 PUBLICATIONS **3,614** CITATIONS
SEE PROFILE

THE JOURNAL OF PHYSICAL CHEMISTRY C

Article

pubs.acs.org/JPCC

Effect of Group-14 and Group-16 Substitution on the Photophysics of Structurally Related Donor−Acceptor Polymers

Gregory L. Gibson, Theresa M. McCormick, and Dwight S. Seferos*

Lash Miller Chemical Laboratories, Department of Chemistry, University of Toronto, 80 St. George Street, Toronto, Ontario M5S 3H6, Canada

Supporting Information

ABSTRACT: A series of eight polymers based on the parent structure, poly[2,6-(4,4-bis-(2-ethylhexyl)-4*H*-cyclopenta[2,1-b;3,4-b′]-dithiophene)-alt-4,7-(2,1,3-benzothiadiazole)] (PCPDTBT), were synthesized for a systematic group-14 and group-16 single atom substitution study. The eight polymers were constructed with C/Si/Ge and S/Se/Te varied in the donor and acceptor, respectively. By examining experimental spectroscopic data and DFT calculated geometry and electronic structure, we gain new physical insights into the effects of heavy atom substitution at different positions in a donor−acceptor polymer. Absorption and emission experiments demonstrate that group-14 substitution in the donor unit only slightly blue shifts the long wavelength absorption (HOMO to LUMO transition) and that group-16 substitution in the acceptor affects this absorption to a much greater extent. Solvatochromism experiments show that the charge transfer excited state is most polarized when the acceptor contains a lighter atom and is influenced very little by the atom in the donor. Changing the atom in the acceptor has less effect on the absorption of the Si-donor and Ge-donor polymers than the C-donor polymers. Polymers that contain C-donors are stronger light absorbers than their Si-donor and Ge-donor analogues regardless of which atom is in the acceptor position. These results clarify the effects of single atom substitution on donor−acceptor polymers and aid in the future design of polymers containing heavy atoms.

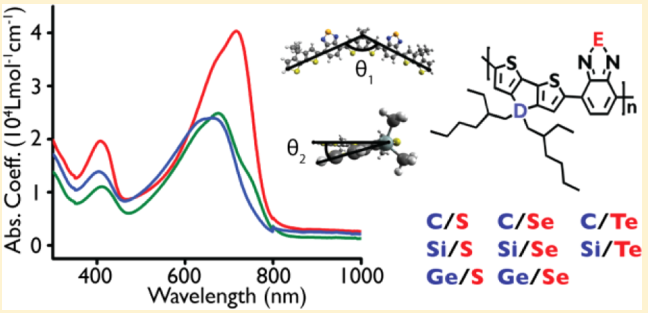

INTRODUCTION

The donor−acceptor (D−A) approach to conjugated polymer design has become a widely used method for preparing conjugated polymers with narrow, tunable highest occupied to lowest unoccupied molecular orbital (HOMO−LUMO) gaps.[1−9] This approach involves synthesizing a polymer with a delocalized π-electron system comprising alternating electron rich (donor) and electron deficient (acceptor) repeat units. In this way, a narrow HOMO−LUMO gap polymer can be constructed by covalently linking the relatively high-lying HOMO level donor unit with the low-lying LUMO level acceptor. The HOMO−LUMO gap can be narrowed or widened based on the structure of the comonomers, and the energy of each can be tuned independently (to some degree) based on donor−acceptor strength and incorporation ratio. This ability to engineer the HOMO−LUMO gap has made these polymers very important semiconductors for use in organic electronic devices.[10−17]

Recently, researchers have described the utility of heavy group-16 atom substitution in the acceptor moiety of prototypical D−A polymers. The earliest examples of this were substitution of S with Se in a 2,1,3-benzothiadiazole that was copolymerized with fluorene[18,19] or phenylene vinylene.[20−22] Following this, 2,1,3-benzoselenadiazole was copolymerized with an alkoxy substituted benzodiothiophene donor[23] as well as an alkylated cyclopentadithiophene donor, 4*H*-cyclopenta[2,1-*b*:3,4-*b*′]-dithiophene (CPDT).[24−27] In each case, the Se-containing polymer exhibited a red-shifted absorption spectrum relative to its S-containing counterpart, resulting from a stabilization of the polymer LUMO level and a destabilization of the polymer HOMO level. These polymers also exhibited a broader absorption spectrum than their S-containing analogues, allowing greater red light absorption, which is advantageous in organic photovoltaic applications. Recently tellurophenes have shown greater long wavelength absorption than their thiophene and selenophene analogues.[28,29] Specifically with regards to D−A polymers, Te substitution in the S position of 2,1,3-benzothiadiazole leads to a further broadening and red shift in the polymer absorption spectrum.[30]

Heavy group-14 atom substitution (typically in the donor unit) has emerged as another key design strategy for D−A polymers. The discovery of siloles as effective electron transport materials[31] led to initial investigation of polymeric silole derivatives in organic light-emitting diodes,[32−34] organic thin film transistors,[35−37] and solar cells.[22,38] In an effort to improve hole transport and red light collection in the solar cell active layer, Si was introduced into the

Received: May 28, 2013
Revised: July 11, 2013
Published: July 17, 2013

dx.doi.org/10.1021/jp405257r | *J. Phys. Chem. C* 2013, 117, 16606−16615

fluorene donor unit of a donor−acceptor copolymer.[39] Subsequently, Si has been incorporated into CPDT.[40,41] Substitution of Si into CPDT and its inclusion in a D−A polymer result in lower polymer HOMO levels and enhanced charge transport in the solid state.[24,26,27] Going a step further, Ge has been incorporated into the bridge position of CPDT in a D−A structure.[42] The resulting Ge-containing polymer has longer wavelength absorption and a higher HOMO level than its Si analogue.

Herein, we present a study in which eight polymers are prepared based on a CPDT donor and a 2,1,3-benzothiadiazole acceptor in an alternating D−A copolymer arrangement. Specifically, Si and Ge are substituted for C in the CPDT donor unit, while Se and Te are substituted for S in the 2,1,3-benzothiadiazole acceptor unit. This allows explicit study of the effect of the plurality of group-14 and group-16 substitution on the photophysics of the polymers. By using optical measurements as well as density functional theory (DFT) and time-dependent DFT (TD-DFT) calculations, we illustrate how and why these substitutions affect the optical properties of a D−A structure.

RESULTS

Synthesis. Eight polymers were synthesized in order to study the effects of group-14 and group-16 substitution on the photophysics of a donor−acceptor polymer with the base structure poly[4,4-bis(2-ethylhexyl)cyclopenta[2,1-b;3,4-b′]dithiophene-2,6-diyl-alt-2,1,3-benzothiadiazole-4,7-diyl] (PCPDTBT) ($\mathbf{P_{CS}}$) (Scheme 1). Each derivative is abbreviated with subscripts that describe the atoms in the donor and acceptor positions. Polymers not containing Te were synthesized by Stille-type condensation polymerization under inert atmosphere using either conventional heating or microwave conditions, as noted in the experimental section. Following polymerization, the reaction mixture was poured into methanol, producing a precipitate that was collected in a Soxhlet thimble and extracted with methanol, hexanes, and chloroform. The solvent was removed from the chloroform fraction to give the target polymer. The Te-acceptor polymers were synthesized from their Se-acceptor analogues by post-polymerization reduction of the acceptor to the diamine and subsequent reoxidation using $TeCl_4$ according to our previously published methodology.[43] The number average molecular weight (M_n) and corresponding PDI values of the previously reported polymers $\mathbf{P_{CS}}$,[44] $\mathbf{P_{CSe}}$,[25] $\mathbf{P_{SiS}}$,[40] and $\mathbf{P_{GeS}}$[42,45] are 14 100 g/mol, 10 300 g/mol, 10 100 g/mol, and 6000 g/mol, and 3.35, 2.50,1.75, and 1.57, respectively. The polymer $\mathbf{P_{CTe}}$ and the new polymer poly[4,4-bis(2-ethylhexyl)dithieno[3,2-*b*;2′,3′-*b*′]-silole-2,6-diyl-*alt*-2,1,3-benzotelluradiazole-4,7-diyl] ($\mathbf{P_{SiTe}}$) are assumed to have an equal degree of polymerization and PDI to their respective Se-acceptor precursors. The new polymers poly[4,4-bis(2-ethylhexyl)dithieno[3,2-*b*;2′,3′-*b*′]silole-2,6-diyl-*alt*-2,1,3-benzoselenadiazole-4,7-diyl] ($\mathbf{P_{SiSe}}$) and poly[4,4-bis(2-ethylhexyl)dithieno[3,2-*b*;2′,3′-*b*′]germole-2,6-diyl-*alt*-2,1,3-benzoselenadiazole-4,7-diyl] ($\mathbf{P_{GeSe}}$) were synthesized in 46% and 62% yield with M_n and PDI values of 11 500 g/mol and 5000 g/mol, and 2.27 and 1.70 respectively. All five known polymers have ^{1}H NMR spectra that are consistent with published reports (Supporting Information). The ^{1}H NMR spectra of the new polymers $\mathbf{P_{SiSe}}$, $\mathbf{P_{SiTe}}$, and $\mathbf{P_{GeSe}}$ have two broad aromatic resonances as well as broad peaks in the alkyl region consistent with the fused-thiophene type donor monomer (Supporting Information). High quality NMR spectra of these polymers are difficult to obtain due to their limited solubility in traditional NMR solvents. Additional characterization data for the polymers were obtained by optical spectroscopy and are described below. The polymer $\mathbf{P_{GeTe}}$ was not able to be synthesized. This is likely due to low solubility of this polymer structure containing both Ge and Te atoms and the reduced stability of the Te-acceptor unit compared with its lighter analogues. Attempts to construct this compound gave material exhibiting irreproducible spectroscopic data.

Optical Properties. The solution absorption spectra of the eight polymers display the dual band absorption typical of a donor−acceptor system (Table 1 and Figure 1).[46] The absorption spectra of the Si-donor polymers $\mathbf{P_{SiS}}$ and $\mathbf{P_{SiSe}}$ show absorption shoulders at approximately 750 and 800 nm, respectively, that are absent in their C- and Ge-donor counterparts as well as their Te-acceptor analogue. $\mathbf{P_{CS}}$ is reported to not adhere to the Beer−Lambert law at high concentrations.[30] This nonlinear behavior is observed at high concentrations for the S-acceptor polymers. To obtain accurate absorption coefficients, Beer−Lambert plots for both the long and short wavelength λ_{max} values were constructed for $\mathbf{P_{CS}}$, $\mathbf{P_{SiS}}$, and $\mathbf{P_{GeS}}$ (Supporting Information, Figures S9−S11). The concentration used to determine the reported absorption coefficients for these polymers was chosen

Scheme 1. (Top) Synthesis of Polymers $\mathbf{P_{CS}}$ (D = C, E = S), $\mathbf{P_{SiS}}$ (D = Si, E = S), $\mathbf{P_{GeS}}$ (D = Ge, E = S), $\mathbf{P_{CSe}}$ (D = C, E = Se), $\mathbf{P_{SiSe}}$ (D = Si, E = Se), $\mathbf{P_{GeSe}}$ (D = Ge, E = Se) by a Stille Coupling Mechanism and (Bottom) Synthesis of Polymers $\mathbf{P_{CTe}}$ (D = C) and $\mathbf{P_{SiTe}}$ (D = Si) by Postpolymerization Modification

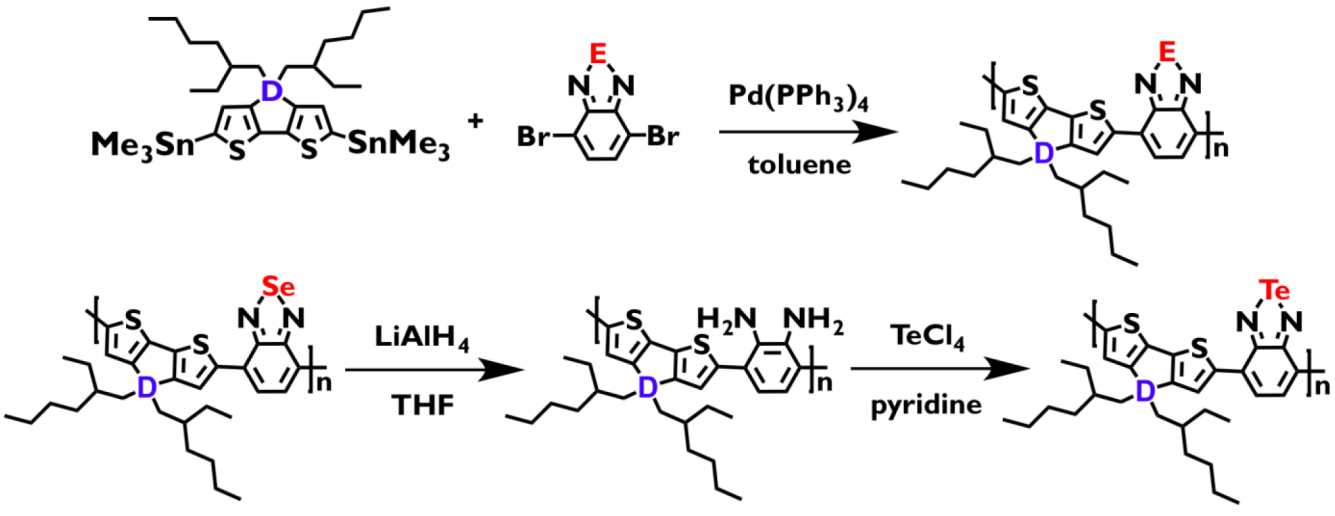

dx.doi.org/10.1021/jp405257r | J. Phys. Chem. C 2013, 117, 16606−16615

Table 1. Experimentally Determined Absorption Coefficients for Long and Short Wavelength Absorption Peaks in Polymer Donor–Acceptor Dual-Band Spectra

	abs λ_{max} [a] (nm) (ε (L mol^{-1}cm^{-1}))	em λ_{max} [b] (nm)
$\mathbf{P_{CS}}$	716 (40300)	767
	408 (19700)	
$\mathbf{P_{CSe}}$	742 (23700)	804
	442 (17200)	
$\mathbf{P_{CTe}}$	785 (9600)	
	448 (13000)	
$\mathbf{P_{SiS}}$	675 (24800)	729
	410 (11000)	
$\mathbf{P_{SiSe}}$	717 (20200)	798
	429 (11500)	
$\mathbf{P_{SiTe}}$	714 (7800)	
	412 (10000)	
$\mathbf{P_{GeS}}$	662 (24000)	730
	405 (13900)	
$\mathbf{P_{GeSe}}$	694 (20000)	795
	422 (13300)	

[a]Recorded in chlorobenzene except for P_{CTe} and P_{SiTe}, which were recorded in dry chloroform. [b]Degassed solutions in chloroform.

from within this linear region. The Se-acceptor polymers display a linear response of absorbance with respect to concentration, and the Te-acceptor polymers are assumed to do so as well. Absorption coefficient values were determined by measuring the absorption spectrum of each polymer in a solution of known concentration prepared with a microbalance and volumetric glassware to ensure accuracy (Table 1). The absorption coefficients were calculated using the molecular weight of the donor–acceptor repeat unit. The spectra used to acquire these values were then plotted (Figure 1).

Changing the donor and acceptor units changes the λ_{max} values and the absorption coefficients of both transitions in the dual band absorption spectrum. First we will present the substitution effects on the long wavelength band and then present those of the short wavelength band.

Comparing polymers with like acceptors (Figure 1A), a blue shift in the λ_{max} of the long wavelength band and a decrease in the magnitude of the absorption coefficient are observed when a lighter group-14 atom is replaced with a heavier one in the donor unit. For S-acceptor $\mathbf{P_{CS}}$, $\mathbf{P_{SiS}}$, and $\mathbf{P_{GeS}}$, the λ_{max} values of the long wavelength band decrease from 716 to 675 to 662 nm, while the absorption coefficient values decrease from 40 300 to 24 800 to 24 000 L mol^{-1} cm^{-1}. The λ_{max} values for the Se-acceptor polymers $\mathbf{P_{CSe}}$, $\mathbf{P_{SiSe}}$, and $\mathbf{P_{GeSe}}$ decrease from 742 to 717 to 694 nm, while the absorption coefficient values are 23 700, 20 200, and 20 000 L mol^{-1} cm^{-1}, respectively. The Ge-donor polymer absorption onsets appear to be blue-shifted relative to their C- and Si-donor analogues, which are nearly identical to each other. The two examples of Te-acceptor polymers display the same pattern. $\mathbf{P_{CTe}}$ has a λ_{max} at 785 nm and a 9600 L mol^{-1} cm^{-1} absorption coefficient, while the analogous values for $\mathbf{P_{SiTe}}$ are 714 nm and 7800 L mol^{-1} cm^{-1}, respectively.

Smaller changes in both λ_{max} values and absorption coefficients are observed in the short wavelength transition, and no obvious trends are apparent on heavy donor atom substitution. This is not unexpected, as the molecular orbitals involved in the short wavelength transition are not greatly dependent on the identity of the acceptor. The λ_{max} values for $\mathbf{P_{CS}}$, $\mathbf{P_{SiS}}$, and $\mathbf{P_{GeS}}$ are 408, 410, and 405 nm, respectively, with corresponding absorption coefficient values of 19 700, 11 000, and 13 900 L mol^{-1} cm^{-1}. In the Se-acceptor case, the λ_{max} values for $\mathbf{P_{CSe}}$, $\mathbf{P_{SiSe}}$, and $\mathbf{P_{GeSe}}$ are 442, 429, and 422 nm, respectively, with corresponding absorption coefficient values of 17 200, 11 500, and 13 300 L mol^{-1} cm^{-1}. A blue shift is observed for $\mathbf{P_{SiTe}}$ relative to $\mathbf{P_{CTe}}$ with λ_{max} values of 412 and 448 nm, respectively. Corresponding absorption coefficients are 13 000 L mol^{-1} cm^{-1} for $\mathbf{P_{CTe}}$ and 10 000 L mol^{-1} cm^{-1} for $\mathbf{P_{SiTe}}$.

To further probe the effect of group-14 and group-16 substitution, we carried out concentration-dependent absorption studies (Figure 2). For the Se-acceptor polymers, the absorption coefficients of both bands are independent of concentration (Figure 2, bottom). However, for the S-acceptor polymers, the absorption coefficients of the long wavelength band are concentration-dependent at concentrations above approximately 3×10^{-6} M (Figure 2, top). We expect the Te-acceptor polymers to behave similarly to the Se-acceptor polymers and to follow the Beer–Lambert law over a wide concentration range.

In order to investigate the effects of group-14 and group-16 substitution on the nature of the long wavelength absorption,

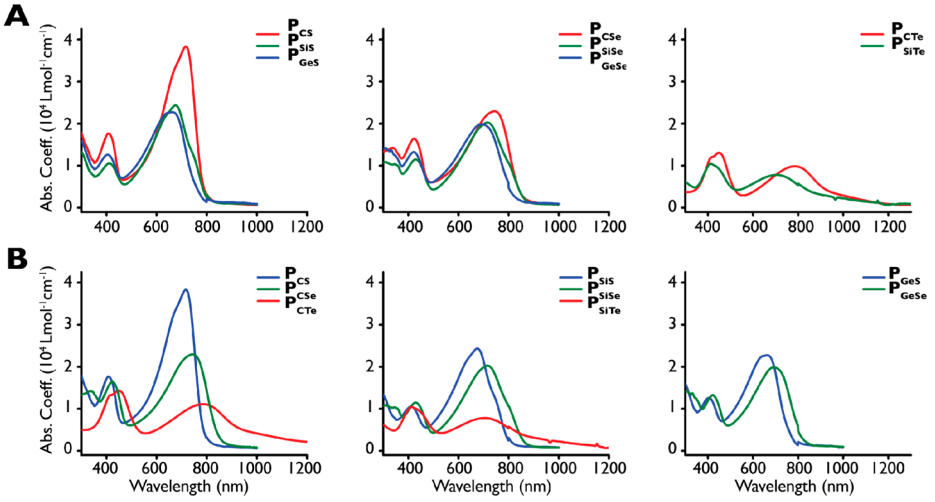

Figure 1. Solution absorption spectra of $\mathbf{P_{CS}}$ (4.07×10^{-7} M), $\mathbf{P_{SiS}}$ (4.94×10^{-6} M), $\mathbf{P_{GeS}}$ (3.70×10^{-6} M), $\mathbf{P_{CSe}}$ (2.95×10^{-6} M), $\mathbf{P_{SiSe}}$ (5.45×10^{-6} M), and $\mathbf{P_{GeSe}}$ (4.87×10^{-6} M) in chlorobenzene, and $\mathbf{P_{CTe}}$ (5.1×10^{-5} M) and $\mathbf{P_{SiTe}}$ (4.6×10^{-6} M) in dry chloroform; (A) spectra plotted by like acceptor in each panel; (B) the same spectra grouped by like donor in each panel.

dx.doi.org/10.1021/jp405257r | J. Phys. Chem. C 2013, 117, 16606–16615

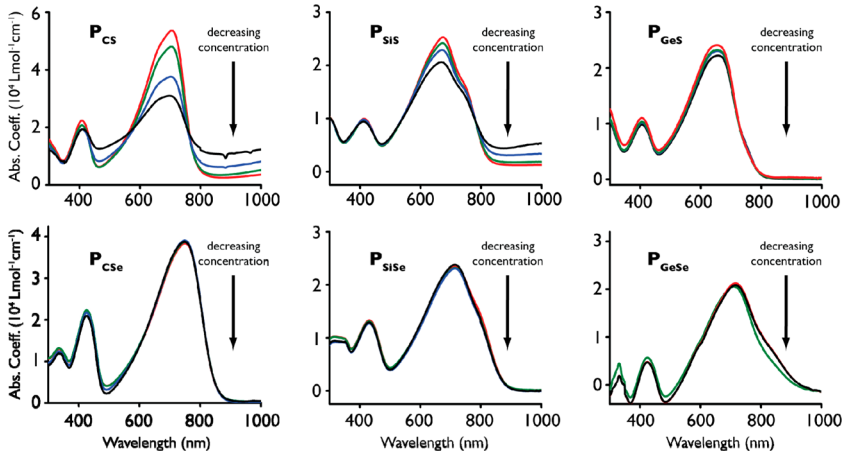

Figure 2. Solution absorption spectra in chloroform at various concentrations. For $\mathbf{P}_{CS}$, concentrations are 3.7×10^{-5}, 1.9×10^{-5}, 9.3×10^{-6}, and 4.7×10^{-6} M. For $\mathbf{P}_{CSe}$, concentrations are 3.9×10^{-5}, 1.6×10^{-5}, 9.1×10^{-6}, and 4.9×10^{-6} M. For $\mathbf{P}_{SiS}$, concentrations are 4.2×10^{-5}, 2.1×10^{-5}, 1.0×10^{-5}, and 5.0×10^{-6} M. For $\mathbf{P}_{SiSe}$, concentrations are 3.3×10^{-5}, 1.7×10^{-5}, 8.4×10^{-6}, and 4.2×10^{-6} M. For $\mathbf{P}_{GeS}$, concentrations are 3.2×10^{-5}, 1.6×10^{-5}, 7.9×10^{-6}, and 4.0×10^{-6} M. For $\mathbf{P}_{GeSe}$, concentrations are 3.2×10^{-6}, 2.1×10^{-6}, and 1.1×10^{-6} M.

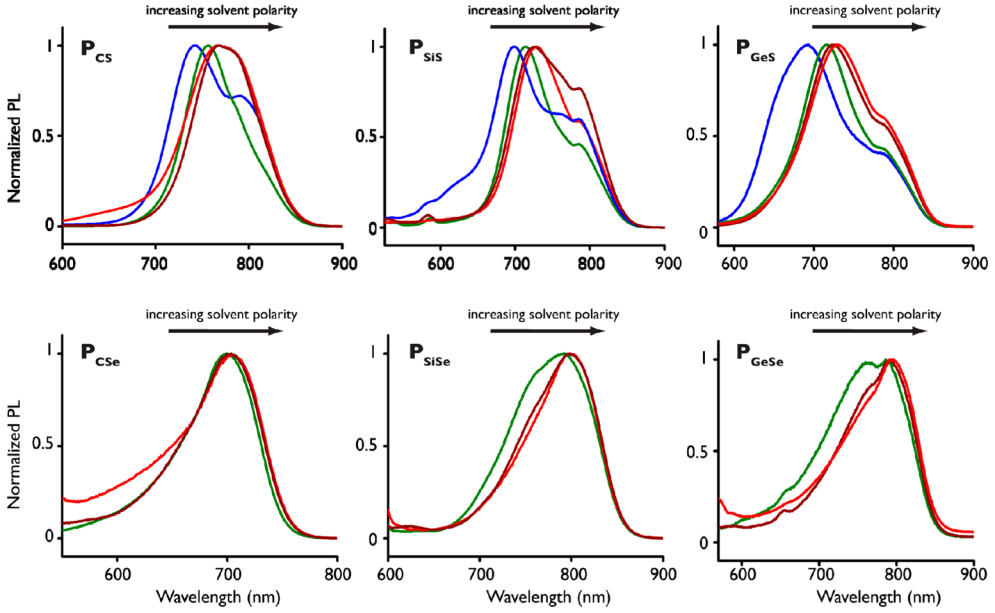

Figure 3. Emission spectra of $\mathbf{P}_{CS}$, $\mathbf{P}_{SiS}$, $\mathbf{P}_{GeS}$, $\mathbf{P}_{CSe}$, $\mathbf{P}_{SiSe}$, and $\mathbf{P}_{GeSe}$ recorded in various solvents. Solvents are cyclohexane (blue), toluene (green), THF (wine), and chloroform (red) and are listed in order of increasing polarity index.

the absorption and emission spectra of the S-acceptor and Se-acceptor polymers were recorded in increasingly polar solvents. The solvents were cyclohexane, toluene, tetrahydrofuran, and chloroform. The Te-acceptor polymers were not sufficiently emissive for spectra to be collected. The absorption spectra λ_{max} values of the six polymers do not change with solvent polarity (Supporting Information, Figure S12). The emission spectra, however, red-shift as the solvent polarity increases (Figure 3, Supporting Information Table S1). The difference in emission λ_{max} between cyclohexane and chloroform is 26 nm for both $\mathbf{P}_{CS}$ and $\mathbf{P}_{SiS}$ and 37 nm for $\mathbf{P}_{GeS}$. A small change in emission λ_{max} values for $\mathbf{P}_{CSe}$, $\mathbf{P}_{SiSe}$, and $\mathbf{P}_{GeSe}$ between toluene and chloroform is observed, 4, 6, and 9 nm respectively. Reliable data for all Se-acceptor polymers in cyclohexane could not be collected because of limited solubility.

Density Functional Theory Calculations. To help elucidate the origin of the features observed in the optical experiments, optimized geometries and orbital energies of eight model compounds were calculated using DFT (Table 2 and Supporting Information Figure S13).[47] The model compounds consist of three donor and two acceptor subunits that are connected in a manner that is analogous to the polymer. Methyl groups were used to approximate the electronic contribution of the 2-ethylhexyl side chains. This structure was chosen to provide insight into the structure of at least one internal donor and one internal acceptor unit in the polymers at a minimal computational cost. The coordinates of the optimized geometries (Supporting Information) and the electronic distribution of the frontier orbitals were calculated using the Gaussian09 program[48] at the CAM-B3LYP[49−51] level of theory with the 6-31G(d) (C, H, N, S, Si, Se) and LANL2DZ (Ge and Te) basis sets. These model compounds are abbreviated analogously to the polymers using **M** in place of **P**.

A number of geometric parameters were calculated on the model compounds to help describe their structure (Table 2). The most notable difference between the optimized geometries

dx.doi.org/10.1021/jp405257r | J. Phys. Chem. C 2013, 117, 16606−16615

Table 2. Selected Calculated Parameters of Model Compounds (CAM-B3LYP; 6-31G(d); LANL2DZ for Ge and Te)[a]

	θ_1 (deg)	average x (Å)	θ_2 (deg)	"D"-thiophene (Å)	HOMO (eV)	LUMO[b] (eV)
$\mathbf{M}_{CS}$	132	4.02	1.4	1.52	−5.79	−3.54
$\mathbf{M}_{SiS}$	110	3.69	5.9	1.88	−5.89	−3.56
$\mathbf{M}_{GeS}$	107	3.65	5.2	1.97	−5.85	−3.53
$\mathbf{M}_{CSe}$	131	4.02	0.4	1.52	−5.73	−3.58
$\mathbf{M}_{SiSe}$	108	3.69	1.9	1.88	−5.83	−3.61
$\mathbf{M}_{GeSe}$	105	3.65	4.7	1.97	−5.81	−3.60
$\mathbf{M}_{CTe}$	129	4.02	3.8	1.52	−5.67	−3.57
$\mathbf{M}_{SiTe}$	106	3.69	2.1	1.88	−5.76	−3.60

[a]See Figure 4 for structures. [b]Calculated by adding the HOMO−LUMO transition energy from the TD-DFT calculation to the HOMO level calculated in the geometry optimization.

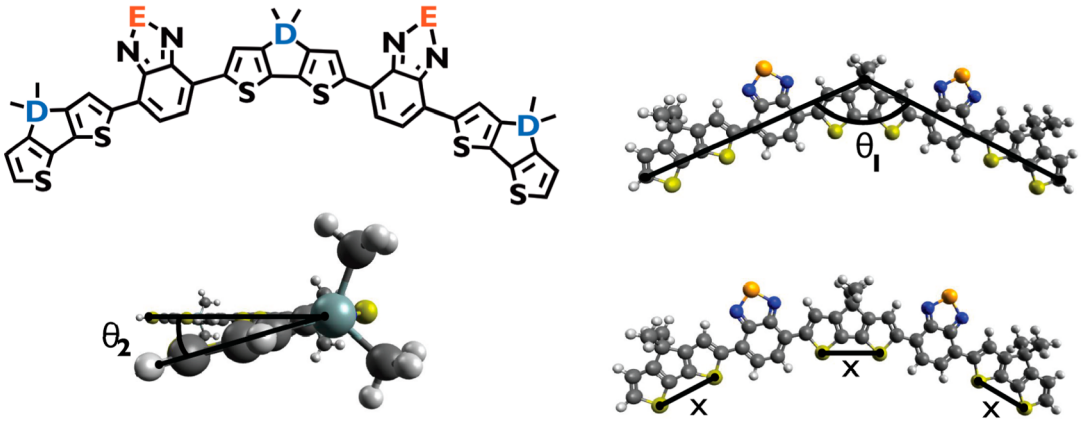

Figure 4. (Top Left) Generic structure of model compounds $\mathbf{M}_{CS}$ (D = C, E = S), $\mathbf{M}_{SiS}$ (D = Si, E = S), $\mathbf{M}_{GeS}$ (D = Ge, E = S), $\mathbf{M}_{CSe}$ (D = C, E = Se), $\mathbf{M}_{SiSe}$ (D = Si, E = Se), $\mathbf{M}_{GeSe}$ (D = Ge, E = Se), $\mathbf{M}_{CTe}$ (D = C, E = Te), and $\mathbf{P}_{SiTe}$ (D = Si, E = Te). (Top Right and Bottom) Optimized geometry of $\mathbf{M}_{SiSe}$ and representative illustrations of geometric parameters calculated on all model compounds (CAM-B3LYP; 6-31G(d); LANL2DZ for Ge and Te).

of the model compounds is their calculated degree of curvature, which we term θ_1 (Figure 4 top right) The curvature increases (θ_1 decreases) by 22−23° between C- and Si-donors and 3° between Si- and Ge-donors. For all model compounds, this increase in curvature coincides with a decrease in the average S−S distance upon group-14 substitution (Table 2 and Figure 4 bottom right). The distance between the donor bridge atom (labeled "D" in Figure 4) and the neighboring thiophene carbons increases from 1.52 to 1.97 Å upon group-14 atom substitution, consistent with a slight rotation of the thiophene units toward each other. This altered geometry of the fused thiophene donor unit produces the more pronounced curvature (decreasing θ_1) in the heavier donor atom-containing model compounds relative to their lighter analogues.

The calculated degree of twist between repeat units also increases upon group-14 substitution (Figure 4 bottom left). The angle θ_2 increases from 1.4° in $\mathbf{M}_{CS}$ to 5.9° in $\mathbf{M}_{SiS}$ and decreases slightly to 5.2° in M_{GeS}. For the Se-acceptor series, however, θ_2 increases from 0.4° in $\mathbf{M}_{CSe}$ to 1.9° in $\mathbf{M}_{SiSe}$ and then increases further to 4.7° in M_{GeSe}. If the angle of twist is extrapolated along the length of a polymer chain, this could result in reduced planarity from one end of the polymer to the other. In the Te-acceptor case, however, θ_2 decreases from 3.8° in $\mathbf{M}_{CTe}$ to 2.1° in $\mathbf{M}_{SiTe}$.

The calculated electronic distribution of the frontier molecular orbitals is similar for all model compounds (Supporting Information, Figure S13). The HOMO is delocalized across the length of the model compound backbone, while the LUMO is more localized on the acceptor units, with a significant portion resting on the S, Se, or Te atom in the benzodiazole ring. The change in the electronic distribution from the HOMO to the LUMO is expected to result in a charge transfer long wavelength absorption. A larger HOMO−LUMO gap is predicted upon group-14 substitution in all acceptor series owing to a stabilization of the polymer HOMO levels (Table 2).

The first ten singlet and triplet excited states of all model compounds were calculated with TD-DFT (Supporting Information, Table S2). The polymer LUMO levels were calculated by adding the energy of the HOMO−LUMO transition from the TD-DFT calculation to the HOMO level predicted in the geometry optimization (Table 2).[52] The TD-DFT calculated absorption spectra were plotted in an analogous manner to the polymer absorption spectra for comparison (Figure 5).

DISCUSSION

As the use of heavy atom substitution in conjugated polymers increases, knowledge of fundamental photophysical effects is a beneficial aid in polymer design. As a starting point, we chose $\mathbf{P}_{CS}$ due to its well-described optical properties. This polymer architecture provides an excellent opportunity to explore examples of group-14 and group-16 substitution effects on the optical properties of a D−A polymer.

The polymers $\mathbf{P}_{CS}$, $\mathbf{P}_{SiS}$, $\mathbf{P}_{CSe}$, and $\mathbf{P}_{SiSe}$ were synthesized with a Stille coupling condensation polymerization yielding polymer with an M_n between 10 000 and 15 000 g/mol. The M_n values of polymers $\mathbf{P}_{GeS}$ and $\mathbf{P}_{GeSe}$ were both below 10 000 g/mol. These lengths are sufficient to saturate each chromophore in solution, allowing molecular-weight independent comparison of the polymers' solution optical properties.[30] As previously reported,[26] greater than 1:1 stoichiometry between donor and

dx.doi.org/10.1021/jp405257r | J. Phys. Chem. C 2013, 117, 16606−16615

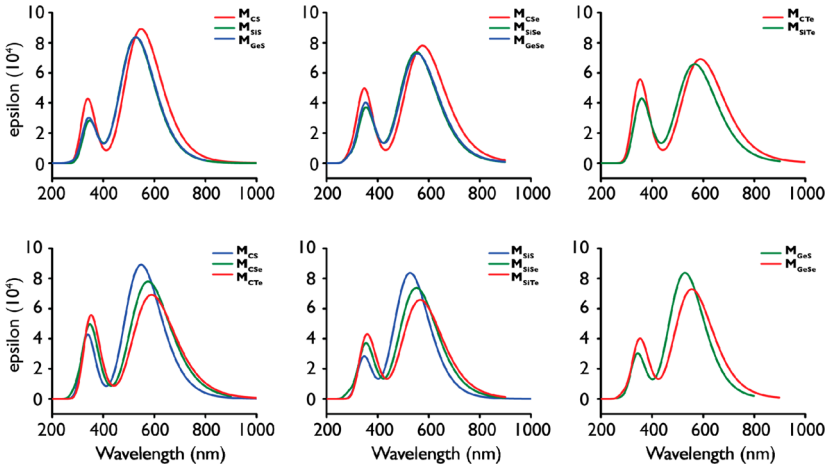

Figure 5. Calculated (TD-DFT) absorption spectra of model compounds; Gaussian functions (0.33 eV full width half-maximum) were applied to each transition (CAM-B3LYP; 6-31G(d); LANL2DZ for Ge and Te).

acceptor (1.05−1.10 equivalents of donor in our case, as noted in the experimental section) are required to account for irremovable impurities in the stannylated monomer and obtain polymers of reasonably high molecular weight. The polymers $\mathbf{P_{CTe}}$ and $\mathbf{P_{SiTe}}$ were synthesized by a postpolymerization methodology, which we have previously reported.[30] The ^{1}H NMR spectra of all polymers have broad resonances that are typical of polymer proton environments (Supporting Information, Figure S1−S8). Both the aromatic and alkyl regions of heavy atom polymer spectra are significantly broader and less detailed than their lighter counterparts, even at higher magnetic field strength, despite their very similar structures. This may be attributable to the lower solubility of heavy atom-containing polymers.

Examination of solution absorption spectra provides insight into the electronic processes in the polymers (Figure 1). D−A polymers typically exhibit a dual-band absorption comprising a long wavelength charge transfer transition and a short wavelength π−π^* transition.[46] This spectral shape appears in the solution absorption spectra of all eight polymers. A charge transfer HOMO−LUMO transition is expected as the calculated HOMOs of all model compounds are distributed across the backbone, while the LUMOs are centered on the acceptor units.

We first describe the effects of group-14 substitution. Focusing on the S acceptor series (Figure 1A) we observe that the intensity of the long wavelength absorption bands decrease for heavier group-14 polymers relative to their lighter counterparts. This effect is most pronounced in the S-acceptor series and is not observed in the calculated absorption spectrum. This may be the result of differences in conformation in the extended polymer chain. As Si and Ge are substituted into the donor unit, the degree of twist (θ_2) of the model compounds increases, as does degree of curvature (θ_1) between the two ends. While the effect of θ_1 is less certain, the effect of θ_2, if extrapolated to a long polymer, indicates a loss of planarity along the backbone of the Si-donor and Ge-donor chains. The lack of planarity in the model compounds suggests a decreased level of conjugation within these polymers, possibly contributing to decreased absorption coefficients relative to their C-donor counterparts.[53] The smaller difference in θ_2 between $\mathbf{M_{SiS}}$ and $\mathbf{M_{GeS}}$ is consistent with the similarity in the long wavelength absorption of their respective polymers. Decreased long wavelength absorption coefficients upon group-14 atom substitution continue for the Se-acceptor and Te-acceptor series. However, the $\mathbf{P_{SiSe}}$ and $\mathbf{P_{GeSe}}$ long wavelength absorptions are very similar, despite much different values of θ_2. Thus, the role of planarity is somewhat less certain as heavier atoms are incorporated into the acceptor units. Trends in the short wavelength band absorption coefficients are less obvious. Regardless of the acceptor atom, the Si-donor and Ge-donor polymer absorption spectra are more similar to each other than to their C-donor analogues, in agreement with the TD-DFT spectra. Overall, the C-donor polymers are the strongest light absorbers in each series regardless of which atom is in the acceptor position.

The lack of planarity in the extended polymer chain may also play a role in the slight blue shift in the long wavelength absorption band that is observed along with group-14 substitution. Decreasing conjugation is known to increase the HOMO−LUMO gap of conjugated molecules.[54] The calculated HOMO and LUMO levels of the model compounds predict this blue shift. The HOMO energy levels of both Si-donor model compounds and Ge-donor model compounds are stabilized relative to their C-donor analogues in all acceptor series. The LUMO energy levels are stabilized to a much lesser degree. This is consistent with the Si stabilizing effect on both the HOMO and LUMO, as observed with siloles.[36] In this case, however, because only the HOMO of a donor−acceptor system is dependent on the donor comonomer, only the HOMO is significantly stabilized by Si, resulting in a slight blue shift of the long wavelength band in the solution absorption spectrum. This stabilizing effect appears to apply to polymers containing the Ge-donor as well.

We now describe the effects of group-16 substitution by focusing on the polymer series with like donors (Figure 1B). Consistent with previous reports, the absorption spectra of all polymers are red-shifted upon substitution with a larger group-16 atom.[30] As previously described, this is likely due to the decreasing ionization energy of the group-16 atom in the acceptor. An exception is observed when comparing $\mathbf{P_{SiSe}}$ and $\mathbf{P_{SiTe}}$. Incorporating Te into the acceptor in this case blue shifts the λ_{max} of $\mathbf{P_{SiTe}}$, although the onset of absorption remains appreciably red-shifted, consistent with a narrowed HOMO−LUMO gap. Generally, the long wavelength absorption is affected to a much greater degree than the short wavelength because of its dependence on the acceptor heteroatom, as shown in the DFT calculated molecular orbital diagrams (Supporting Information, Figure S13). The red shifts of both long and short wavelength absorption bands are consistent with the TD-DFT calculated absorption spectra.

dx.doi.org/10.1021/jp405257r | J. Phys. Chem. C 2013, 117, 16606−16615

Focusing on the donor series, the absorption coefficients for the C-donor series are influenced by the acceptor atom to a greater extent than in either the Si- or Ge-donor series. This is observed as a lesser decrease in magnitude of the Si- and Ge-series absorption coefficients upon Se-acceptor substitution. This difference may be due to the greater polarizability of the Si and Ge atoms relative to C. Greater polarizability enhances the heavier atom's ability to donate electron density to the weaker, less electron-poor Se-acceptor, minimizing the effect of replacing S with Se on the long wavelength band intensity. Group-16 substitution appears to have little effect on the absorption coefficients of the short wavelength absorptions. This is consistent with the $\pi-\pi^*$ nature of this transition centralized on the donor unit, in which the acceptor heteroatom plays little role.

Among all of the absorption spectra, we observe slight shoulders in the long wavelength bands of the Si-donor polymers $\mathbf{P}_{\mathbf{SiS}}$ and $\mathbf{P}_{\mathbf{SiSe}}$ in every solvent tested (Figure 1 and Supporting Information Figure S12) as well as in the polymers $\mathbf{P}_{\mathbf{GeS}}$ and $\mathbf{P}_{\mathbf{GeSe}}$ in cyclohexane only. In the case of $\mathbf{P}_{\mathbf{SiS}}$, these absorption shoulders have been previously reported and are thought to result from efficient π-stacking.[24,26,40] Shoulders are noticeably absent from the calculated absorption spectra of the Si-donor and Ge-donor polymers (Figure 5), supporting the claim that these shoulders result from supramolecular interaction. Interestingly, these shoulders do not appear in the spectra of $\mathbf{P}_{\mathbf{SiTe}}$ or in the spectra of the Ge-donor polymers in solvents other than cyclohexane. Given the relatively poor solubility of the Ge-donor polymers in cyclohexane, these shoulders could result from aggregation in this poor solvent. Polymer aggregation is consistent with the report that these shoulders are enhanced in film absorption spectra of $\mathbf{P}_{\mathbf{SiS}}$.[24,40]

Concentration-dependent absorption spectra reveal that the long wavelength absorption coefficients of the S-acceptor polymers $\mathbf{P}_{\mathbf{CS}}$, $\mathbf{P}_{\mathbf{SiS}}$, and $\mathbf{P}_{\mathbf{GeS}}$ are concentration dependent above 10^{-6} M, while the short wavelength coefficients are not (Figure 2). This effect is most pronounced in the spectra of $\mathbf{P}_{\mathbf{CS}}$ and less so as heavier group-14 atoms are introduced. The Se-acceptor series absorption coefficients do not show this same concentration dependence. Because this concentration effect on the long wavelength transition is only observed in the S-acceptor series, along with a corresponding increase in the spectra baseline absorption, we speculate both features are caused by an intermolecular effect, possibly owing to the increased electronegativity of the S atom. At high dilution, this concentration dependence disappears, and the absorption adheres to the Beer–Lambert law (Supporting Information Figures S9–S11). Importantly, the disappearance of this concentration dependence allows us to calculate absorption coefficients at the λ_{max} for the short and long wavelength absorptions in the S-acceptor series and compare the spectra of all eight polymers.

Further highlighting the effect of the S-acceptor, the absorption spectra (Supporting Information, Figure S15) and emission spectra (Figure 3) of the non-Te containing polymers were recorded in increasingly polar solvents. $\mathbf{P}_{\mathbf{CTe}}$ and $\mathbf{P}_{\mathbf{SiTe}}$ were not examined due to limited solubility and solution stability. As solvent polarity increases, the absorption λ_{max} values do not change, while there is an observable red shift in the emission λ_{max} of all six polymers. This is consistent with a charge transfer excited state contributing to the long wavelength absorption. After photon absorption and promotion of an electron to the polymer LUMO, a polar solvent stabilizes the polar excited state before emission occurs, resulting in an increasingly large Stokes shift. This red shift is greater in the S-acceptor series (Figure 3, top) than in the Se-acceptor series (Figure 3, bottom). This demonstrates that polymers with S-acceptors have a more polar excited state then their Se-acceptor analogues regardless of which donor is used and that the identity of the acceptor strongly influences the polarity of the excited state. Another feature unique to the S-acceptor series is an emission shoulder, red-shifted from the main peak. This shoulder appears weakest in toluene, the lone aromatic solvent. It is possible that these shoulders result from lower energy states accessed through polymer aggregation in a more polar solvent.

CONCLUSIONS

A series of eight polymers was synthesized by Stille coupling condensation and postpolymerization modification to allow for a systematic group-14 and group-16 single atom substitution study on a donor–acceptor polymer. The polymers were constructed with C/Si/Ge varied in the donor structure, while S/Se/Te were varied in the acceptor. The Si–Se, Ge–Se, and Si–Te analogues are new and are examples of donor–acceptor polymers that contain both a heavy group-14 and group-16 atom in their repeat unit. By examining the experimental optical and DFT calculated properties of these substituted polymers, we are able to gain new physical insight into heavy atom substitution in conjugated polymer systems. (i) Heavier group-14 atom substitution in the donor leads to a slight blue shift in the long wavelength absorption band. (ii) The identity of the acceptor affects the polymer HOMO–LUMO gap to a much greater degree than the donor. (iii) The charge-transfer is strongest when the acceptor contains a S atom and is not influenced by heavy atom substitution in the donor. (iv) Heavier acceptors have smaller absorption coefficients; however, this is lessened when the donor is also heavy, for example, in the case of the Si-donor and Ge-donor polymers. (v) Polymers that contain the C-donor are stronger light absorbers than those that contain the Si- or Ge-donors regardless of which atom is in the acceptor position, and of these, the C–S analogue is the strongest light absorber of the polymers studied here. These results provide guidance for the design of future donor–acceptor polymers that contain heavy atoms.

EXPERIMENTAL SECTION

General Considerations. Unless stated otherwise, starting materials were purchased and used as received. 4,4′-Bis(2-ethylhexyl)-5,5′-dibromo-dithieno[3,2-b:2′,3′-d]silole was purchased from Solarmer Materials, Inc. Deuterated chloroform was purchased from Cambridge Isotope Laboratories, freeze–pump–thaw degassed, and dried on 4 Å molecular sieves. All other chemicals were purchased from Sigma-Aldrich. Pyridine was dried by refluxing over $CaCl_2$ before distilling under nitrogen. 4,7-Dibromo-2,1,3-benzoselenadiazole,[19] 4,4′-bis(2-ethyl-hexyl)-5,5′-bis(trimethyltin)-dithieno[3,2-b:2′,3′-d]silole,[40] and 4,4′-bis-(2-ethyl-hexyl)-5,5′-bis(trimethyltin)-dithieno[3,2-b:2′,3′-d]-germole[42,45] were prepared by literature procedures. Poly[(4,4′-bis(2-ethylhexyl)cyclopenta[2,1-b;3,4-b′]dithiophene-2,6-diyl-alt-2,1,3-benzotelluradiazole)-4,7-diyl] was prepared as previously reported by us.[30] Unless otherwise noted, all manipulations involving air- or water-sensitive reagents were performed under a dry nitrogen atmosphere using standard Schlenk techniques or in a nitrogen-filled glovebox. Solvents were degassed by bubbling with nitrogen for 25 min and dried using an Innovative Technologies solvent purification system. NMR spectra were recorded on a Varian Mercury 400 spectrometer operating at 400 MHz for ^{1}H or on an Agilent DD2 500 spectrometer operating at 500 MHz for ^{1}H,

dx.doi.org/10.1021/jp405257r | J. Phys. Chem. C 2013, 117, 16606–16615

as noted. Chemical shifts are reported in ppm at ambient temperature. ^{1}H chemical shifts are referenced to the residual protonated chloroform peak at 7.26 ppm. Absorption spectra were recorded on a Varian Cary 5000 UV−vis−NIR spectrophotometer in chloroform or chlorobenzene, as noted, at ∼0.01 mg/mL. Emission spectra were recorded on a Photon Technology International QuantaMaster 40-F NA spectrofluorometer in chloroform, THF, toluene, and cyclohexane as indicated. Polymer molecular weights were determined with a Viscotek HT-GPC (1,2,4-trichlorobenzene, 140 °C) using Tosoh Bioscience LLC TSK-GEL GMH$_{HR}$-HT mixed-bed columns and narrow molecular weight distribution polystyrene standards.

Density Functional Theory Calculations. Geometry optimizations were performed using the Gaussian09 program[48] employing the Becke Three Parameter Hybrid Functionals Lee−Yang−Parr (B3LYP)[49,50] including Handy and co-workers' long-range corrected version of B3LYP using the Coulomb-attenuating method (CAM-B3LYP).[51] The standard 6-31G(d) basis set was used for C, H, N, S, Si, and Se atoms; the LANL2DZ basis set was used for Ge and Te.[55] Starting geometries were generated using Gaussview05.[48] A frequency calculation was preformed on the optimized geometries to make sure a local minimum was found. Time-dependent DFT (TD-DFT)[47] calculations were carried out from the optimized geometries with the same basis sets used for geometry optimizations; the first ten singlet and triplet states were calculated.

Synthesis and Characterization. *Poly[(4,4′-bis(2-ethylhexyl)cyclopenta[2,1-b;3,4-b′]dithiophene-2,6-diyl-alt-2,1,3-benzothiadiazole)-4,7-diyl],* ***P$_{CS}$.*** In a nitrogen-filled glovebox, 4,7-dibromo-2,1,3-benzothiadiazole (37.0 mg, 0.129 mmol), 4,4′-bis(2-ethyl-hexyl)-5,5′-bis(trimethyltin)-dithieno-[3,2-b:2′,3′-d]silole (102 mg, 0.137 mmol), tetrakis-triphenylphosphinepalladium(0) (7 mg, 0.006 mmol), and dry toluene (4 mL) were added to a 25 mL Teflon-capped storage flask. The flask was removed and placed onto a Schlenk line and degassed by three freeze−pump−thaw cycles before being sealed and heated to 130 °C in an oil bath for 24 h. After being allowed to cool, the dark blue mixture was poured out into methanol (50 mL) and filtered through a Soxhlet thimble. The solid was extracted successively with methanol, hexanes, and chloroform until each fraction is colorless. The solid recovered from the chloroform fraction was passed through a plug of silica eluting with further chloroform to give a dark blue solid (38 mg, 0.071 mmol, 54%). ^{1}H NMR (400 MHz, $CDCl_3$) δ: 8.14 (m, 2H), 7.88 (br s, 2H), 2.07 (br s, 4H), 1.02 (br s, 18H), 0.88 (br s, 6H), 0.68 (br s, 6H). GPC: M_n = 14 100 g/mol, M_w = 47 200 g/mol, PDI = 3.35.

Poly[(4,4′-bis(2-ethylhexyl)cyclopenta[2,1-b;3,4-b′]-dithiophene-2,6-diyl-alt-2,1,3-benzoselenadiazole)-4,7-diyl], ***P$_{CSe}$.*** In a nitrogen-filled glovebox, 4,7-dibromo-2,1,3-benzoselenadiazole (43.0 mg, 0.129 mmol), 4,4′-bis(2-ethyl-hexyl)-5,5′-bis(trimethyltin)-dithieno[3,2-b:2′,3′-d]silole (102 mg, 0.137 mmol), tetrakis-triphenylphosphinepalladium(0) (7 mg, 0.006 mmol), and dry toluene (4 mL) were added to a 25 mL Teflon-capped storage flask. The flask was removed and placed onto a Schlenk line and degassed by three freeze−pump−thaw cycles before being sealed and heated to 130 °C in an oil bath for 24 h. After being allowed to cool, the dark green mixture was poured out into methanol (50 mL) and filtered through a Soxhlet thimble. The solid was extracted successively with methanol, hexanes, and chloroform until each fraction is colorless. The solid recovered from the chloroform fraction was passed through a plug of silica eluting with further chloroform to give a dark green solid (39 mg, 0.067 mmol, 54%). ^{1}H NMR (400 MHz, $CDCl_3$) δ: 8.02 (br m, 2H), 7.79 (br s, 2H), 2.05 (br s, 4H), 1.02 (br s, 16H), 0.88 (br s, 2H), 0.68 (br s, 12H). GPC: M_n = 10 000 g/mol, M_w = 25 700 g/mol, PDI = 2.50.

Poly[(4,4′-bis(2-ethylhexyl)dithieno[3,2-b:2′,3′-d]silole)-2,6-diyl-alt-(2,1,3-benzothia diazole)-4,7-diyl], ***P$_{SiS}$.*** In a nitrogen-filled glovebox, 4,7-dibromo-2,1,3-benzothiadiazole (44.0 mg, 0.150 mmol), 4,4′-bis(2-ethyl-hexyl)-5,5′-bis(trimethyltin)-dithieno[3,2-b:2′,3′-d]silole (118 mg, 0.159 mmol), tetrakis-triphenylphosphinepalladium(0) (8 mg, 0.007 mmol), and dry toluene (4 mL) were added to a 25 mL Teflon-capped storage flask. The flask was removed and placed onto a Schlenk line and degassed by three freeze−pump−thaw cycles before being sealed and heated to 130 °C in an oil bath for 24 h. After being allowed to cool, the dark blue mixture was poured out into methanol (50 mL) and filtered through a Soxhlet thimble. The solid was extracted successively with methanol, hexanes, and chloroform until each fraction is colorless. The solid recovered from the chloroform fraction was passed through a plug of silica eluting with further chloroform to give a dark blue solid (31 mg, 0.056 mmol, 38%). ^{1}H NMR (500 MHz, $CDCl_3$) δ: 8.50−7.50 (br m, 4H), 2.07 (br s, 2H), 1.50−1.00 (br m, 20H), 1.00−0.80 (br m, 12H). GPC: M_n = 10 000 g/mol, M_w = 17 500 g/mol, PDI = 1.75.

Poly[(4,4′-bis(2-ethylhexyl)dithieno[3,2-b:2′,3′-d]silole)-2,6-diyl-alt-(2,1,3-benzoselena diazole)-4,7-diyl], ***P$_{SiSe}$.*** In a nitrogen-filled glovebox, 4,7-dibromo-2,1,3-benzoselenadiazole (43.0 mg, 0.126 mmol), 4,4′-bis(2-ethyl-hexyl)-5,5′-bis-(trimethyltin)-dithieno[3,2-b:2′,3′-d]silole (102 mg, 0.137 mmol), tetrakis-triphenylphosphinepalladium(0) (7 mg, 0.006 mmol), and dry toluene (4 mL) were added to a 25 mL Teflon-capped storage flask. The flask was removed and placed onto a Schlenk line and degassed by three freeze−pump−thaw cycles before being sealed and heated to 130 °C in an oil bath for 24 h. After being allowed to cool, the dark green mixture was poured out into methanol (50 mL) and filtered through a Soxhlet thimble. The solid was extracted successively with methanol, hexanes, and chloroform until each fraction is colorless. The solid recovered from the chloroform fraction was passed through a plug of silica eluting with further chloroform to give a dark green solid (35 mg, 0.059 mmol, 46%). ^{1}H NMR (500 MHz, $CDCl_3$) δ: 8.25−7.50 (br m, 4H), 2.07 (br s, 2H), 1.50−1.00 (br m, 20H), 1.00−0.80 (br m, 12H). GPC: M_n = 11 500 g/mol, M_w = 26 200 g/mol, PDI = 2.27.

Poly[(4,4′-bis(2-ethylhexyl)dithieno[3,2-b:2′,3′-d]-germole)-2,6-diyl-alt-(2,1,3-benzothiadiazole)-4,7-diyl], ***P$_{GeS}$.*** In a nitrogen-filled glovebox, 4,7-dibromo-2,1,3-benzothiadiazole (19 mg, 0.065 mmol), 4,4′-bis(2-ethyl-hexyl)-5,5′-bis-(trimethyltin)-dithieno[3,2-b:2′,3′-d]germole (55 mg, 0.070 mmol), tetrakis-triphenylphosphinepalladium(0) (4 mg, 0.003 mmol), and dry toluene (2 mL) were added to a 5 mL Biotage microwave reactor vial. The vial was placed in a microwave reactor and heated to 120 °C for 2 min, 140 °C for 2 min, and 170 °C for 60 min. After being allowed to cool, the dark blue mixture was poured out into methanol (25 mL) and filtered through a Soxhlet thimble. The solid was extracted successively with methanol, hexanes, and chloroform until each fraction ran colorless. The solid recovered from the chloroform fraction was passed through a short silica column eluting with chloroform to afford a dark blue solid (15 mg, 0.024 mmol, 36%). ^{1}H NMR (500 MHz, $CDCl_3$) δ: 8.20 (br s, 2H), 7.86 (br s, 2H), 1.26 (br s, 16H), 0.85 (br s, 18H). GPC: M_n = 6000 g/mol, M_w = 9500 g/mol, PDI = 1.56.

Poly[(4,4′-bis(2-ethylhexyl)dithieno[3,2-b:2′,3′-d]-germole)-2,6-diyl-alt-(2,1,3-benzoselenadiazole)-4,7-diyl], ***P$_{GeSe}$.*** In a nitrogen-filled glovebox, 4,7-dibromo-2,1,3-benzoselenadiazole (49.5 mg, 0.145 mmol), 4,4′-bis(2-ethyl-hexyl)-5,5′-bis(trimethyltin)-dithieno[3,2-b:2′,3′-d]germole (120 mg,

0.0152 mmol), tetrakis-triphenylphosphinepalladium(0) (8 mg, 0.007 mmol), and dry toluene (2 mL) were added to a 5 mL Biotage microwave reactor vial. The vial was placed in a microwave reactor and heated to 120 °C for 2 min, 140 °C for 2 min, and 170 °C for 60 min. After being allowed to cool, the dark blue mixture was poured out into methanol (25 mL) and filtered through a Soxhlet thimble. The solid was extracted successively with methanol, hexanes, and chloroform until each fraction ran colorless. The solid recovered from the chloroform fraction was passed through a short silica column eluting with chloroform to afford a dark green solid (58 mg, 0.090 mmol, 62%). ^{1}H NMR (500 MHz, $CDCl_3$) δ: 8.10 (br s, 2H), 7.80 (br s, 2H), 1.31 (br m, 4H), 0.84 (br s, 18H). GPC: M_n = 5000 g/mol, M_w = 7700 g/mol, PDI = 1.70.

Poly[(4,4′-bis(2-ethylhexyl)dithieno[3,2-b:2′,3′-d]silole)-2,6-diyl-alt-2,3-diaminobenzo-4,7-diyl]. Poly[(4,4′-bis(2-ethylhexyl)dithieno[3,2-b:2′,3′-d]silole)-2,6-diyl-alt-2,1,3-benzoselenadiazole-4,7-diyl] (99.6 mg, 0.166 mmol) was placed in a 100 mL Schlenk flask under nitrogen with dry THF (15 mL). Lithium aluminum hydride (75.0 mg, 1.98 mmol) was added under nitrogen, and the resulting mixture was stirred at room temperature for 16 h. The mixture was poured into water (20 mL), extracted with chloroform (3 × 20 mL), and further washed with water (20 mL). The mixture was dried on magnesium sulfate, and the solvent was removed by rotary evaporation to give a dark red solid (65 mg, 0.124 mmol, 75%), which was used without further purification.

Poly[(4,4′-bis(2-ethylhexyl)dithieno[3,2-b:2′,3′-d]silole)-2,6-diyl-alt-2,1,3-benzotellurodiazole-4,7-diyl], P_{SiTe}. Poly[(4,4′-bis(2-ethylhexyl)dithieno[3,2-b:2′,3′-d]silole)-2,6-diyl-alt-2,3-diaminobenzo-4,7-diyl] (65.0 mg, 0.124 mmol) was placed in a 25 mL Schlenk flask under nitrogen with dry pyridine (7 mL). Tellurium(IV)chloride (60.0 mg, 0.20 mmol) was added under nitrogen, and the resulting mixture was stirred at room temperature for 16 h. Dry methanol (10 mL) was added to the mixture by cannula, the mixture was stirred for 5 min, and the solvent was decanted by cannula filter. This procedure was repeated 3 times before residual methanol was removed under vacuum to give a dark green solid (39 mg, 0.065 mmol, 52%). ^{1}H NMR (400 MHz, $CDCl_3$) δ: 8.63 (s, 2H), 7.70 (s, 2H), 1.63 (br s, 4H), 1.02 (br s, 20H), 0.83 (br s, 10H).

■ ASSOCIATED CONTENT

Ⓢ Supporting Information

^{1}H NMR spectra; Beer−Lambert plots; solvatochromism absorption spectra; emission peak data; additional DFT data; and optimized geometry coordinates. This material is available free of charge via the Internet at http://pubs.acs.org.

■ AUTHOR INFORMATION

Notes

The authors declare no competing financial interest.

■ ACKNOWLEDGMENTS

This work was supported by the University of Toronto, NSERC, the CFI, and the Ontario Research Fund. G.L.G. thanks the Xerox Research Centre of Canada for a Graduate Award and the University of Toronto Department of Chemistry for the Jim Guillet Chemistry Graduate Scholarship.

■ REFERENCES

(1) Havinga, E.; ten Hoeve, W.; Wynberg, H. A New Class of Small Band Gap Organic Polymer Conductors. *Polym. Bull.* **1992**, *29*, 119−126.
(2) Havinga, E.; ten Hoeve, W.; Wynberg, H. Alternate Donor-Acceptor Small-Band-Gap Semiconducting Polymers; Polysquaraines and Polycroconaines. *Synth. Met.* **1993**, *55*, 299−306.
(3) Zhang, M.; Tsao, H. N.; Pisula, W.; Yang, C.; Mishra, A. K.; Müllen, K. Field-Effect Transistors Based on a Benzothiadiazole−Cyclopentadithiophene Copolymer. *J. Am. Chem. Soc.* **2007**, *129*, 3472−3473.
(4) Zhou, E.; Nakamura, M.; Nishizawa, T.; Zhang, Y.; Wei, Q.; Tajima, K.; Yang, C.; Hashimoto, K. Synthesis and Photovoltaic Properties of a Novel Low Band Gap Polymer Based on N-Substituted Dithieno[3,2-b:2′,3′-d]pyrrole. *Macromolecules* **2008**, *41*, 8302−8305.
(5) Wang, E.; Ma, Z.; Zhang, Z.; Vandewal, K.; Henriksson, P.; Inganäs, O.; Zhang, F.; Andersson, M. R. An Easily Accessible Isoindigo-Based Polymer for High-Performance Polymer Solar Cells. *J. Am. Chem. Soc.* **2011**, *133*, 14244−14247.
(6) Burkhart, B.; Khlyabich, P.; Canak, T.; LaJoie, T.; Thompson, B. C. "Semi-Random" Multichromophoric rr-P3HT Analogues for Solar Photon Harvesting. *Macromolecules* **2011**, *44*, 1242−1246.
(7) Bundgaard, E.; Krebs, F. C. Low-Band-Gap Conjugated Polymers Based on Thiophene, Benzothiadiazole, and Benzobis(thiadiazole). *Macromolecules* **2006**, *39*, 2823−2831.
(8) Jenekhe, S. A.; Lu, L.; Alam, M. M. New Conjugated Polymers with Donor−Acceptor Architectures: Synthesis and Photophysics of Carbazole−Quinoline and Phenothiazine−Quinoline Copolymers and Oligomers Exhibiting Large Intramolecular Charge Transfer. *Macromolecules* **2001**, *34*, 7315−7324.
(9) Guo, X.; Watson, M. D. Pyromellitic Diimide-Based Donor−Acceptor Poly(phenylene ethynylene)s. *Macromolecules* **2011**, *44*, 6711−6716.
(10) Öktem, G.; Balan, A.; Baran, D.; Toppare, L. Donor−Acceptor Type Random Copolymers for Full Visible Light Absorption. *Chem. Commun.* **2011**, *47*, 3933−3935.
(11) Sonmez, G.; Shen, C. K.; Rubin, Y.; Wudl, F. A Red, Green, and Blue (RGB) Polymeric Electrochromic Device (PECD): the Dawning of the PECD Era. *Angew. Chem.* **2004**, *116*, 1524−1528.
(12) Hains, A. W.; Liang, Z.; Woodhouse, M. A.; Gregg, B. A. Molecular Semiconductors in Organic Photovoltaic Cells. *Chem. Rev.* **2010**, *110*, 6689−6735.
(13) Beaujuge, P. M.; Subbiah, J.; Choudhury, K. R.; Ellinger, S.; McCarley, T. D.; So, F.; Reynolds, J. R. Green Dioxythiophene-Benzothiadiazole Donor−Acceptor Copolymers for Photovoltaic Device Applications. *Chem. Mater.* **2010**, *22*, 2093−2106.
(14) Jellison, J. L.; Lee, C.-H.; Zhu, X.; Wood, J. D.; Plunkett, K. N. Electron Acceptors Based on an All-Carbon Donor−Acceptor Copolymer. *Angew. Chem., Int. Ed.* **2012**, *51*, 12321−12324.
(15) Wood, J. D.; Jellison, J. L.; Finke, A. D.; Wang, L.; Plunkett, K. N. Electron Acceptors Based on Functionalizable Cyclopenta[hi]-aceanthrylenes and Dicyclopenta[de,mn]tetracenes. *J. Am. Chem. Soc.* **2012**, *134*, 15783−15789.
(16) Fu, B.; Baltazar, J.; Hu, Z.; Chien, A.-T.; Kumar, S.; Henderson, C. L.; Collard, D. M.; Reichmanis, E. High Charge Carrier Mobility, Low Band Gap Donor−Acceptor Benzothiadiazole−Oligothiophene Based Polymeric Semiconductors. *Chem. Mater.* **2012**, *24*, 4123−4133.
(17) Tao, Y.; McCulloch, B.; Kim, S.; Segalman, R. A. The Relationship between Morphology and Performance of Donor−Acceptor Rod−Coil Block Copolymer Solar Cells. *Soft Matter* **2009**, *5*, 4219−4230.
(18) Yang, R.; Tian, R.; Hou, Q.; Yang, W.; Cao, Y. Synthesis and Optical and Electroluminescent Properties of Novel Conjugated Copolymers Derived from Fluorene and Benzoselenadiazole. *Macromolecules* **2003**, *36*, 7453−7460.
(19) Yang, R.; Tian, R.; Yan, J.; Zhang, Y.; Yang, J.; Hou, Q.; Yang, W.; Zhang, C.; Cao, Y. Deep-Red Electroluminescent Polymers: Synthesis and Characterization of New Low-Band-Gap Conjugated Copolymers for Light-Emitting Diodes and Photovoltaic Devices. *Macromolecules* **2005**, *38*, 244−253.

(20) Chen, J.; Cao, Y. Silole-Containing Polymers: Chemistry and Optoelectronic Properties. *Macromol. Rapid Commun.* **2007**, *28*, 1714−1742.
(21) Li, X.; Zeng, W.; Xia, Y.; Yang, W.; Cao, Y. Synthesis and Properties of Novel Deep Red-Emitting Copolymers Based on a Poly(*p*-phenylenevinylene) Derivative. *J. Appl. Polym. Sci.* **2006**, *102*, 4321−4327.
(22) Wang, E.; Wang, L.; Lan, L.; Luo, C.; Zhuang, W.; Peng, J.; Cao, Y. High-Performance Polymer Heterojunction Solar Cells of a Polysilafluorene Derivative. *Appl. Phys. Lett.* **2008**, *92*, 033307.
(23) Hou, Y.; Chen, Y.; Liu, Q.; Yang, M.; Wan, X.; Yin, S.; Yu, A. A Novel Tetrathiafulvalene (TTF)-Fused Poly(aryleneethynylene) with an Acceptor Main Chain and Donor Side Chains: Intramolecular Charge Transfer (CT), Stacking Structure, and Photovoltaic Property. *Macromolecules* **2008**, *41*, 3114−3119.
(24) Scharber, M. C.; Koppe, M.; Gao, J.; Cordella, F.; Loi, M. A.; Denk, P.; Morana, M.; Egelhaaf, H.-J.; Forberich, K.; Dennler, G.; Gaudiana, R.; Waller, D.; Zhu, Z.; Shi, X.; Brabec, C. J. Influence of the Bridging Atom on the Performance of a Low-Bandgap Bulk Heterojunction Solar Cell. *Adv. Mater.* **2010**, *22*, 367−370.
(25) Hou, J.; Chen, T. L.; Zhang, S.; Yang, Y. Poly[4,4-bis(2-ethylhexyl)cyclopenta[2,1-b;3,4-b′]dithiophene-2,6-diyl- alt-2,1,3-benzoselenadiazole-4,7-diyl], a New Low Band Gap Polymer in Polymer Solar Cells. *J. Phys. Chem. C* **2009**, *113*, 1601−1605.
(26) Coffin, R. C.; Peet, J.; Rogers, J.; Bazan, G. C. Streamlined Microwave-Assisted Preparation of Narrow-Bandgap Conjugated Polymers for High-Performance Bulk Heterojunction Solar Cells. *Nat. Chem.* **2009**, *1*, 657−661.
(27) Chen, H.-Y.; Hou, J.; Hayden, A. E.; Yang, H.; Houk, K. N.; Yang, Y. Silicon Atom Substitution Enhances Interchain Packing in a Thiophene-Based Polymer System. *Adv. Mater.* **2010**, *22*, 371−375.
(28) Jahnke, A. A.; Howe, G. W.; Seferos, D. S. Polytellurophenes with Properties Controlled by Tellurium-Coordination. *Angew. Chem., Int. Ed.* **2010**, *49*, 10140−10144.
(29) McCormick, T. M.; Jahnke, A. A.; Lough, A. J.; Seferos, D. S. Tellurophenes with Delocalized π-Systems and Their Extended Valence Adducts. *J. Am. Chem. Soc.* **2012**, *134*, 3542−3548.
(30) Gibson, G. L.; McCormick, T. M.; Seferos, D. S. Atomistic Band Gap Engineering in Donor−Acceptor Polymers. *J. Am. Chem. Soc.* **2012**, *134*, 539−547.
(31) Tamao, K.; Uchida, M.; Izumizawa, T.; Furukawa, K.; Yamaguchi, S. Silole Derivatives As Efficient Electron Transporting Materials. *J. Am. Chem. Soc.* **1996**, *118*, 11974−11975.
(32) Liu, M. S.; Luo, J.; Jen, A. K.-Y. Efficient Green-Light-Emitting Diodes from Silole-Containing Copolymers. *Chem. Mater.* **2003**, *15*, 3496−3500.
(33) Chen, J.; Peng, H.; Law, C. C. W.; Dong, Y.; Lam, J. W. Y.; Williams, I. D.; Tang, B. Z. Hyperbranched Poly(phenylenesilolene)s: Synthesis, Thermal Stability, Electronic Conjugation, Optical Power Limiting, and Cooling-Enhanced Light Emission. *Macromolecules* **2003**, *36*, 4319−4327.
(34) Chen, J.; Law, C. C. W.; Lam, J. W. Y.; Dong, Y.; Lo, S. M. F.; Williams, I. D.; Zhu, D.; Tang, B. Z. Synthesis, Light Emission, Nanoaggregation, and Restricted Intramolecular Rotation of 1,1-Substituted 2,3,4,5-Tetraphenylsiloles. *Chem. Mater.* **2003**, *15*, 1535−1546.
(35) Wang, F.; Luo, J.; Yang, K.; Chen, J.; Huang, F.; Cao, Y. Conjugated Fluorene and Silole Copolymers: Synthesis, Characterization, Electronic Transition, Light Emission, Photovoltaic Cell, and Field Effect Hole Mobility. *Macromolecules* **2005**, *38*, 2253−2260.
(36) Lu, G.; Usta, H.; Risko, C.; Wang, L.; Facchetti, A.; Ratner, M. A.; Marks, T. J. Synthesis, Characterization, and Transistor Response of Semiconducting Silole Polymers with Substantial Hole Mobility and Air Stability. Experiment and Theory. *J. Am. Chem. Soc.* **2008**, *130*, 7670−7685.
(37) Beaujuge, P. M.; Pisula, W.; Tsao, H. N.; Ellinger, S.; Müllen, K.; Reynolds, J. R. Tailoring Structure−Property Relationships in Dithienosilole−Benzothiadiazole Donor−Acceptor Copolymers. *J. Am. Chem. Soc.* **2009**, *131*, 7514−7515.
(38) Mi, B.; Dong, Y.; Li, Z.; Lam, J. W. Y.; Häußler, M.; Sung, H. H. Y.; Kwok, H. S.; Dong, Y.; Williams, I. D.; Liu, Y.; Luo, Y.; Shuai, Z.; Zhu, D.; Tang, B. Z. Making Silole Photovoltaically Active by Attaching Carbazolyl Donor Groups to the Silolyl Acceptor Core. *Chem. Commun.* **2005**, 3583−3585.
(39) Boudreault, P.-L. T.; Michaud, A.; Leclerc, M. A New Poly(2,7-Dibenzosilole) Derivative in Polymer Solar Cells. *Macromol. Rapid Commun.* **2007**, *28*, 2176−2179.
(40) Hou, J.; Chen, H.-Y.; Zhang, S.; Li, G.; Yang, Y. Synthesis, Characterization, and Photovoltaic Properties of a Low Band Gap Polymer Based on Silole-Containing Polythiophenes and 2,1,3-Benzothiadiazole. *J. Am. Chem. Soc.* **2008**, *130*, 16144−16145.
(41) Henson, Z. B.; Welch, G. C.; van der Poll, T.; Bazan, G. C. Pyridalthiadiazole-Based Narrow Band Gap Chromophores. *J. Am. Chem. Soc.* **2012**, *134*, 3766−3779.
(42) Amb, C. M.; Chen, S.; Graham, K. R.; Subbiah, J.; Small, C. E.; So, F.; Reynolds, J. R. Dithienogermole As a Fused Electron Donor in Bulk Heterojunction Solar Cells. *J. Am. Chem. Soc.* **2011**, *133*, 10062−10065.
(43) Gibson, G.; McCormick, T.; Seferos, D. Atomistic Band Gap Engineering in Donor Acceptor Polymers. *Polym. Prepr.* **2012**, *53*, 21−22.
(44) Mühlbacher, D.; Scharber, M.; Morana, M.; Zhu, Z.; Waller, D.; Gaudiana, R.; Brabec, C. High Photovoltaic Performance of a Low-Bandgap Polymer. *Adv. Mater.* **2006**, *18*, 2884−2889.
(45) Gendron, D.; Morin, P.-O.; Berrouard, P.; Allard, N.; Aïch, B. R.; Garon, C. N.; Tao, Y.; Leclerc, M. Synthesis and Photovoltaic Properties of Poly(dithieno[3,2-b:2′,3′-d]germole) Derivatives. *Macromolecules* **2011**, *44*, 7188−7193.
(46) Beaujuge, P. M.; Amb, C. M.; Reynolds, J. R. Spectral Engineering in π-Conjugated Polymers with Intramolecular Donor−Acceptor Interactions. *Acc. Chem. Res.* **2010**, *43*, 1396−1407.
(47) Bauernschmitt, R.; Ahlrichs, R. Treatment of Electronic Excitations within the Adiabatic Approximation of Time Dependent Density Functional Theory. *Chem. Phys. Lett.* **1996**, *256*, 454−464.
(48) Frisch, M.; et al. *Gaussian 09*; Gaussian, Inc.: Wallingford, CT, 2009.
(49) Becke, A. D. Density-Functional Thermochemistry. IV. A New Dynamical Correlation Functional and Implications for Exact-Exchange Mixing. *J. Chem. Phys.* **1996**, *104*, 1040−1046.
(50) Becke, A. D. Density-Functional Thermochemistry. III. The Role of Exact Exchange. *J. Chem. Phys.* **1993**, *98*, 5648−5652.
(51) Yanai, T.; Tew, D.; Handy, N. A New Hybrid Exchange-Correlation Functional Using the Coulomb-Attenuating Method (CAM-B3LYP). *Chem. Phys. Lett.* **2004**, *393*, 51−57.
(52) McCormick, T. M.; Bridges, C. R.; Carrera, E. I.; DiCarmine, P. M.; Gibson, G. L.; Hollinger, J.; Kozycz, L. M.; Seferos, D. S. Conjugated Polymers: Evaluating DFT Methods for More Accurate Orbital Energy Modeling. *Macromolecules* **2013**, *46*, 3879−3886.
(53) Maddux, T.; Li, W.; Yu, L. Stepwise Synthesis of Substituted Oligo(phenylenevinylene) via an Orthogonal Approach. *J. Am. Chem. Soc.* **1997**, *119*, 844−845.
(54) Streifel, B. C.; Peart, P. A.; Martínez Hardigree, J. F.; Katz, H. E.; Tovar, J. D. Torsional Influences within Disordered Organic Electronic Materials Based upon Non-Benzenoid 1,6-Methano[10]annulene Rings. *Macromolecules* **2012**, *45*, 7339−7349.
(55) Hay, P. J.; Wadt, W. R. Ab Initio Effective Core Potentials for Molecular Calculations. Potentials for the Transition Metal Atoms Sc to Hg. *J. Chem. Phys.* **1985**, *82*, 270−283.